Jantsch S, Helfield JM, Bodensteiner L, Sobocinski KL, Bunn AG. 2025. A characterization of hyporheic temperatures with applications for salmon habitat restoration in a thermally impaired river. Northwest Science 98(2): *in press.*

Sydney Jantsch, Natural Resources Department, Lummi Nation, 2665 Kwina Rd., Bellingham, Washington 98226,

James M. Helfield[1], Department of Environmental Sciences, Western Washington University, 516 High St., Bellingham, Washington 98225,

Leo Bodensteiner, Department of Environmental Sciences, Western Washington University, 516 High St., Bellingham, Washington 98225,

Kathryn L. Sobocinski, Department of Environmental Sciences, Western Washington University, 516 High St., Bellingham, Washington 98225,

and

Andrew G. Bunn, Department of Environmental Sciences, Western Washington University, 516 High St., Bellingham, Washington 98225

A Characterization of Hyporheic Temperatures with Applications for Salmon Habitat Restoration in a Thermally Impaired River

Running footer: Characterization of Hyporheic Temperatures

2 tables, 4 figures

[1] Author to whom correspondence should be addressed. Email: helfiej@wwu.edu

Abstract

Elevated stream temperatures represent an important stress affecting Pacific salmon (*Oncorhynchus* spp.). In thermally-impaired streams, upwellings of shallow subsurface (i.e., hyporheic) water have the potential to create patches of cool-water refuge that allow salmon to persist in otherwise unsuitable water temperatures. Since patterns of hyporheic upwelling are influenced by variations in streambed topography, habitat restoration actions such as engineered log jam construction may be used to preserve or promote upwellings. This strategy requires that hyporheic flows remain cooler in summer, relative to the overlying surface stream, but this might not always be the case. Here we characterize the relationship between hyporheic and overlying surface temperatures during a summer low-flow season in a restored reach of the South Fork Nooksack River. Among six sampling sites, we found that one had hyporheic temperatures that were consistently colder than the overlying surface stream, two had hyporheic temperatures that were variable but more moderate than those of the overlying surface stream, and three had hyporheic temperatures that were not cooler or more stable than those of the overlying surface stream. Habitat mapping suggests that thermally stable hyporheic flow paths may be associated with specific combinations of channel geomorphic units, which influence flow path length, depth and discharge. These findings may be used to identify potential areas of cool-water refuge and guide the design and placement of habitat restoration actions to promote climate adaptation for salmon populations in thermally-impaired streams.

Key Points

- Upwellings of cool, subsurface water have the potential to provide summertime refuge for salmon in rivers that are otherwise too warm.
- Not all upwellings are cool enough to benefit salmon.

- Habitat mapping can be used to identify locations with cool upwellings and guide salmon habitat restoration efforts.

Keywords: hyporheic, river, salmon, temperature

Introduction

Pacific salmon (*Oncorhynchus* spp.) have been described as keystone species because of their importance as a food resource for predators and scavengers (Cederholm et al. 1989, Hilderbrand et al. 1999, Ford et al. 2010) and because of their role in transporting marine-derived nutrients to freshwater and terrestrial ecosystems (Willson et al. 1998, Lundberg and Moberg 2003, Helfield and Naiman 2006). Pacific salmon also play a crucial role as cultural keystone species for Native Nations of the Pacific Northwest, and declines in salmon abundance threaten the physical, social, economic, and spiritual well-being of Indigenous communities (Newell 1994, Carothers et al. 2021). Over the past century, human actions have caused significant declines in salmon populations, and despite considerable efforts and expenditures for conservation and restoration, the prospects for salmon recovery remain unclear (Schoonmaker et al. 2003, Gustafson et al. 2007, Lackey 2022). Several populations of Pacific salmon continue to be listed as threatened or endangered under terms of the U.S. Endangered Species Act (NOAA 2015) and Canada's Species at Risk Act (DFO 2018).

Elevated stream temperatures represent a major stressor affecting salmon populations and contribute to the impairment of numerous riverine ecosystems in the Pacific Northwest (Hashim and Bresler 2005, USEPA 2021). Elevated stream temperatures are caused by anthropogenic factors such as deforestation, water diversion, and urbanization, which entail reductions in shade and decreased infiltration of precipitation into groundwater (Poole and Berman 2001). This impairment will become increasingly severe and widespread in the coming years due to global climate change, the effects of which include rising air temperatures as well as earlier and faster snowmelt and changes in streamflow generation, resulting in decreased summertime discharge (Mote et al. 2003, van Vliet et al. 2011). As lower flows entail decreased thermal inertia (Booker and Whitehead 2022), these hydrologic changes exert an important influence on stream temperatures, exacerbating the warming effects of rising air temperatures and loss of shade.

With regard to salmon, thermal impairment refers to the occurrence of warm water temperatures that are outside the optimal range for performance. Temperature affects salmon at all life history stages. In incubating embryos, warmer stream temperatures increase the rate of development and alter the timing of emergence, with potentially adverse effects on survival rates (Bjornn and Reiser 1991). In fry, excessively warm temperatures (⪆ 25 °C) can result in acute mortality, while warm sublethal temperatures (⪆ 15 °C) affect standard and active metabolism so as to restrict the amount of energy that can be used for swimming and feeding, which hampers growth and makes fry more vulnerable to predators (McCullough et al. 2001). In returning adults, elevated temperatures induce stress responses and increase the virulence of pathogens, both of which can lead to premature mortality (von Biela et al. 2020). The latter effects are especially important in populations that undertake spawning migrations in summer, such as Sockeye Salmon (*O. nerka*; Hinch and Martins 2011) and early (i.e., spring- and summer-run) Chinook Salmon (*O. tshawytscha*; Connor et al. 2019, Bowen et al. 2020).

A strategy that shows promise for allowing salmon populations to persist in thermally-impaired streams involves the construction of engineered log jams to create pool habitat. Engineered log jams are human-made structures made of wood and other materials installed in streams to simulate naturally-occurring large woody debris (LWD), which fulfills several critical functions affecting fish habitat (Beechie and Sibley 1997, Gregory et al. 2003). In degraded streams, engineered log jams are frequently designed to deflect streamflow, which scours the adjacent streambed and enhances the development of deep, complex pools (Roni et al. 2008, Cramer 2012). Among other habitat benefits, deep wood-formed pools have greater thermal inertia and thus maintain cooler and more stable summertime temperatures relative to other habitat features (Elliott 2000), providing thermally-favorable holding water (i.e., cool-water refuge) for salmon. Access to such cool-water refuge can mitigate thermal stress sufficiently to improve growth and survival rates in juvenile salmon (Ebersole et al. 2001, 2003) and improve reproductive success in migrating adults (Benda et al. 2015). By allowing salmon to persist in thermally-impaired streams, engineered log jams may promote climate adaptation in threatened populations and serve as an essential component of a comprehensive strategy for salmon recovery.

Engineered log jams may be most effective at providing cool-water refuge when wood-formed pools receive inputs from cool-water sources such as subsurface upwellings. At sites where such cool-water sources are not present, the log jams themselves can alter the shape of the riverbed in a way that invites the potential for localized upwellings of cool water from the hyporheic zone. The hyporheic zone comprises saturated sediments beneath and beside a stream channel containing some portion of water from the surface stream (Edwards 1998). In comparison with overlying surface stream flows, hyporheic flows tend to be more thermally stable (i.e., experience less extreme seasonal and diel fluctuations in temperature), and hyporheic inputs can thus moderate stream temperatures (Burkholder et al. 2008, Torgersen et al. 2012). In coarse-bedded alluvial rivers during the summer low-flow season, a large proportion of total discharge may be carried through the hyporheic zone (Fernald et al. 2006), and significant amounts of water may be exchanged between the hyporheic zone and the overlying surface stream. Hyporheic exchange is strongly influenced by streambed topography: Areas of upwelling, where water moves from the hyporheic zone to the surface stream, typically occur at the heads of pools, while areas of downwelling, where water moves from the surface stream into the hyporheic zone, typically occur at pool tailouts (Harvey and Bencala 1993, Edwards 1998).

Spatial patterns and volumes of hyporheic exchange can thus be drastically altered by changes in bed topography (Kasahara and Wondzell 2003, Tonina and Buffington 2007), which can be brought about by naturally-occurring LWD accumulations or engineered log jams. Previous studies have demonstrated that in-stream structures may promote localized upwellings that can influence stream temperatures (Mutz et al. 2007, Hester and Doyle 2008, Hester et al. 2009, Wondzell et al. 2009, Sawyer and Cardenas 2012, Menichino and Hester 2014, Bilski et al. 2022). These findings suggest that engineered log jams may be used to induce hyporheic upwellings to create patches of cool-water refuge for salmon, but this strategy will only be effective where hyporheic flow paths are cooler than the surface stream.

The specific objective of this research is to assess spatial and temporal variation in the relationship between hyporheic and overlying surface temperatures during the summer low-flow season within a thermally-impaired stream reach. In so doing, we aim to elucidate the extent to which hyporheic upwellings can deliver cool water to log jam-formed pools and provide cool-water refuge for salmon. The long-term goal of this work is to guide future habitat restoration efforts to promote climate resiliency in salmon populations threatened by elevated stream temperatures.

Methods

Study Sites

The South Fork Nooksack River (SF Nooksack) is an 80 km (50 mi)-long tributary of the Nooksack River in northwestern Washington state, USA. Its Nooksack place name is *Nuxw7íyem*, which translates as "always clear water" (NNR 2012). It drains approximately 425 km^2 (164 mi^2) of watershed area before it meets with the North Fork Nooksack River, the northernmost river in Washington, to form the main stem of the Nooksack River (Grah et al.

2017). The headwaters of the SF Nooksack arise > 1,829 m (6,000 ft) in elevation above the confluence with the North Fork in snowfields on Twin Sisters Mountain, *Kwetl'kwítl' Smánit*, the melting of which sustains river flows throughout the beginning of the summer. This winter mountain snowpack generally melts fully in June and July, after which river flow is sustained primarily by groundwater inflow (Gendaszek 2014, Grah et al. 2017). River flows typically decrease throughout August and early September, and it is during this low-flow period that water temperatures are typically warmest (USGS 2024). As a consequence of climate change, the North Cascades are experiencing lower amounts of snowfall, and the snowpack on the Twin Sisters is melting faster each year (Grah et al. 2017). The combination of decreased snowpack, earlier melt-off, and rising summer air temperatures leads to a prolonged low-flow season with diminished water flows and increasing water temperatures, a condition that is likely to be exacerbated in years to come (Yoder and Raymond 2022).

Predominant land uses in the SF Nooksack basin are logging in the headwaters with agricultural operations in the lower reaches, where streamside forest clearing has resulted in decreased shading and correspondingly increased water temperatures (Grah et al. 2017). The lack of riparian buffer also contributes to a scarcity of LWD and LWD-formed pools, with a corresponding scarcity of cool-water refuge habitat (Maudlin et al. 2002, Soicher et al. 2006). The surficial geology of the lower river valley consists of an unconfined aquifer within post-Vashon glacial outwash and alluvium (Gendaszek 2014). The streambed is composed mainly of sand, gravel and cobble alluvium, with some boulders and exposed bedrock. Coarse-scale measurements indicate the presence of hydraulically conductive substrates with ample potential for hyporheic exchange (Gendaszek 2014).

The SF Nooksack supports all seven North American species of Pacific salmon (USEPA

2016a). Chinook Salmon spawning has been observed 51 river km (32 river miles) upstream of the confluence with the North Fork Nooksack River (Pelto et al. 2022). The lower SF Nooksack is a priority area for salmon habitat restoration (WRIA 1 SRB 2005) because it supports an endangered population of early Chinook Salmon that is considered essential for the recovery of the broader Puget Sound Chinook Salmon evolutionarily significant unit (ESU), which is listed as threatened under the U.S. Endangered Species Act (ESA; Maudlin et al. 2002, Soicher et al. 2006, Butcher et al. 2016, USEPA 2016b). The SF Nooksack early Chinook Salmon enter the river as adults in spring and spawn in mid-August through September, holding for long periods when river temperatures are at their warmest (Maudlin et al. 2002). As a consequence, the population is imperiled by elevated stream temperatures that are exacerbated by low flows during the summer (Grah et al. 2017).

Data for this project were collected in the Nesset's Reach section of the lower SF Nooksack (48.692019 ° N, -122.164114 ° W). Nesset's Reach is approximately 2.7 km (1.67 miles) long, located near Acme, Washington, approximately 17 river km (10 river miles) above the confluence with the North Fork Nooksack River. In 2016 and 2018, the Nooksack Indian Tribe Natural Resources Department (NNR) installed a series of engineered log jams in Nesset's Reach (NNR 2015, NNR 2016). The principal objective of the NNR Nesset's Reach restoration project was to provide cool-water refuge for adult early Chinook Salmon by creating deep and complex scour pools.

Experimental Design and Data Collection

We measured water temperature simultaneously in the hyporheic zone and the overlying surface stream at six sampling sites within Nesset's Reach. Each site consisted of a single engineered log jam and its associated wood-formed pool, with a riffle immediately upstream. Each site was assigned an identification number that corresponded to the NNR-assigned identification number of the engineered log jam, with higher numbers indicating positions further downstream (Table 1). All temperatures were measured using temperature loggers with ± 0.2 °C precision (TidBiT v2 Temp logger, Onset Computer Corporation, Bourne, MA). At each site, hyporheic temperatures were measured with a single logger deployed inside a piezometer at a depth of approximately 35 cm below the streambed. The piezometer was located in an upwelling zone at the transition from the riffle tail to the pool head. The corresponding surface stream temperatures were measured with a second logger deployed on the streambed < 1 m upstream of the piezometer. The two loggers were programmed to record water temperature simultaneously every hour during the summer low-flow season (August 6 – September 13, 2022) at each site.

Each piezometer consisted of a 1.2–1.5 m length of schedule 40 polyvinyl chloride (PVC) pipe with an outside diameter of 4.2 cm and an inside diameter of 3.5 cm (nominal size 1 ¼”). Each piezometer was plugged at the bottom and had 14 holes in the sidewall that were 0.3175 cm (1/8”) in diameter. The holes were equally spaced over the bottom 10 cm of the piezometer’s length, allowing hyporheic water to flow through the piezometer. The holes were covered with a fine (200-μm) mesh sleeve to reduce sediment inputs inside the piezometer. To facilitate measurements of installation depth, the piezometers were graduated and labeled.

We used a variation of the apparatus and procedures described by Baxter et al. (2003) to install the piezometers into the substrate. We used a 1.2 m-long driving rod made of 4.4 cm-diameter (nominal size 1 ¾”) cold-rolled steel fitted with a 6 cm-diameter steel cap, and a 1.14 m-long driving sleeve made of stainless-steel pipe with an inside diameter of 4.6 cm and an outside diameter of 5.1 cm (nominal size 2”). For each piezometer, the driving rod was inserted into the sleeve, and the rod and sleeve were pounded into the substrate together using a 1.8-kg

(4-lb.) sledgehammer. Once driven down to the appropriate depth, the rod was removed from inside the sleeve, and a piezometer was inserted in its place. The sleeve was then removed from around the piezometer, leaving the piezometer inserted into the substrate. Precise installation depths were measured and recorded for each piezometer (Table 1).

At some sites, we found it necessary to use open-bottom piezometers with no sidewall perforations, into which we inserted a 2.5 cm-diameter steel driving rod with a 6 cm-diameter steel cap and pounded on the cap to drive the rod and piezometer into the substrate simultaneously. This process was faster, required fewer field materials, and was less likely to result in sand or silt being lodged between the driving rod and sleeve, which inhibited piezometer installation at some sites. The open-bottom piezometers measured hydraulic head at the bottom opening of the piezometer, approximately 35 cm below the streambed, over an area equal to that of a circle with a diameter equal to the piezometer's inside diameter (i.e., 9.62 cm^2). In contrast, the perforated, closed-bottom piezometers integrated hydraulic head measurements within a column of water extending 10 cm above the bottom of the piezometer, approximately 25–35 cm below the streambed. This column was equal in volume to the length of the sidewall perforations multiplied by the inside area of the piezometer (i.e., 10 cm x 9.62 cm^2 = 96.2 cm^3). This difference in piezometer apparatus may have had a subtle effect on hydraulic head measurements, but it likely did not affect hyporheic temperature measurements, as temperatures were measured at comparable depths at the bottoms of both closed- and open-bottomed piezometers. The closed-bottom piezometers were deployed at two of the six study sites (1302 and 2124), and the open-bottom piezometers were used at the other four sites (1306, 1312, 1313, and 1316).

Following installation, we used a hand-held vacuum pump (Mityvac model MV8000, SKF Lubrication Systems USA Inc., St. Louis, MO) to remove water and fine sediment inside the piezometer. For each piezometer, pumping continued until ≥ 2 L of water had been removed and the pumped water was visibly clear. This was to remove any surface water that may have entered the piezometer during installation and to ensure a connection with the hyporheic zone.

We measured temperatures at the riffle/pool transition at each site because this location has the greatest potential of being in an upwelling zone (Harvey and Bencala 1993, Edwards 1998). This was to ensure that temperature measurements were collected in upwelling or neutral (i.e., neither upwelling nor downwelling) areas, which contain greater proportions of subsurface flow, as opposed to downwelling areas, which contain greater proportions of recent surface stream water. After the piezometer was left to equilibrate for 24 hours, we measured the upwelling potential at the installation location. Upwelling potential was characterized in terms of vertical hydraulic gradient (VHG), which is a unitless measure of the pressure differential between the hyporheic zone at a given location and the overlying surface stream (Dahm and Valett 1996). VHG is calculated as follows:

$$\text{VHG} = (h_s - h_p) / L$$

where h_s is the height of the top of the piezometer above the water level of the surface stream (cm), h_p is the height of the top of the piezometer above the water level within the piezometer (cm), and L is the depth from the streambed to the first opening in the piezometer (cm). Positive VHG values indicate upwelling potential, negative VHG values indicate downwelling potential, and a zero VHG value indicates neutral conditions (Dahm and Valett 1996). We used an electronic water level meter (Model 102M Mini Water Level Meter, Solinst Canada Ltd., Georgetown, ON) to measure h_s and h_p. To account for fluctuations in surface water level due to turbulent streamflow, we measured h_s inside a 3.5 cm-diameter stilling well (i.e., a length of open-bottomed PVC pipe) attached to the outside of the piezometer, extending vertically from the top of the piezometer to a depth below the stream surface but above the streambed. Table 1 lists VHG values observed at each site and piezometer installation depths.

At each site, once we confirmed that upwellings were present, we installed a temperature logger at the bottom of the piezometer. We then installed another temperature logger on the streambed < 1 m upstream from the piezometer. Each streambed temperature logger was housed inside a short (5–8 cm) length of 4 cm-diameter (nominal 1 ¼”) schedule 40 PVC, which was perforated all over to allow water flow. This housing was then placed inside a 30–35 cm length of 8.9 cm-diameter (nominal 3”) schedule 40 PVC conduit that was also perforated all over and filled with river rocks that acted as an anchor to keep the logger in place throughout the season. Once assembled and placed on the streambed, each PVC housing was covered with river rocks for camouflage. Periodically, we visited the sites to confirm that the piezometers and streambed housings were still in position. During that time, we used a data shuttle (HOBO Waterproof Shuttle, Onset Computer Corporation, Bourne, MA) to download the data collected thus far.

To help identify geomorphic factors that might influence patterns of hyporheic temperature, we measured thalweg depths and surveyed channel geomorphic units throughout Nesset’s Reach. These habitat surveys were conducted during the low-flow season (August 2022), following NNR protocols for monitoring habitat restoration projects (Coe 2019).

Data Analysis

We used permutation tests to assess the difference in mean temperature between the hyporheic zone and the surface stream for each hour of the day at each site. A permutation test evaluates the statistical significance of an observed difference by comparing it to a null distribution generated by randomly shuffling the data between categories or treatments to break any inherent relationships (Manly 2007). First, hourly temperatures were averaged across all days in the sample period to capture a representative diel pattern. For each hour at each site, we then calculated the observed difference in temperature between the hyporheic zone and the surface stream. This observed difference was then compared to a null distribution of differences generated by permuting the site-specific temperature values between the hyporheic and surface stream categories 1,000 times. The p-value for each hour was calculated as the proportion of permuted differences equal to or greater than the observed difference. Differences were considered statistically significant if fewer than 5% of permutations produced a value as extreme as the observed difference, corresponding to a significance threshold of $\alpha = 0.05$.

We characterized the hyporheic and surface temperature regimes at each site in terms of daily maximum and daily range. Daily maximum was calculated as the maximum temperature recorded during a given 24-hour period (00:00–23:59), and daily range was calculated as the difference between the daily maximum and minimum temperature recorded during a given 24-hour period. To account for the potential influence of extreme temperature days on daily maximum values, we also calculated the seven-day average of the daily maximum (7DADM), a moving average in which the daily maximum temperature value for a given day was averaged with the daily maximum values of the previous three days and the following three days. We calculated the difference in means and performed pairwise one-tailed t-tests with a Bonferroni-adjusted significance level of $\alpha = 0.0167$ (0.05/3) at each site to assess differences in these response variables between the hyporheic zone and the overlying surface stream. Shapiro-Wilks tests indicated that the data met assumptions of normality ($p < 0.05$). We used linear regression models across all sites to assess the extent to which temperature response variables were confounded by VHG or installation depth. All analyses were conducted in R version 4.2.2 (R

Core Team 2023).

Results and Discussion

The relationship between hyporheic temperature and overlying surface stream temperature is variable over small spatial scales. Not all sites featured hyporheic flows that were cooler or more thermally stable than the overlying surface stream during the summer low-flow season (Figure 1). Permutation tests indicate that the diel relationship between hyporheic and overlying surface stream temperature varies among sites (Table 2). At site 1316, the hyporheic zone was significantly cooler at every hour of the day. At sites 1302 and 1306, the hyporheic zone was significantly cooler during part of the day. At site 1302, the hyporheic zone was cooler for the majority of the day (i.e., 10:00–02:00), and at site 1306 the hyporheic zone was cooler throughout the morning (05:00–11:00) and in the afternoon and evening (14:00–21:00), but not at mid-day. In contrast, at sites 1312, 1313, and 2124 there were no significant differences in temperature between the hyporheic zone and the surface stream at any hour of the day. Using terms defined by Arrigoni et al. (2008), the diel temperature cycles that we observed may be characterized as follows: At site 1316, hyporheic flow is cooled (i.e., exhibits cooler mean temperatures) and buffered (i.e., exhibits a dampened range of temperatures) relative to surface flow; at site 1302, hyporheic flow is also cooled and buffered, although to a lesser extent; and at site 1306 hyporheic flow is buffered and somewhat lagged (i.e., exhibits a difference in phase, with peaks and troughs occurring slightly after those occurring in the surface stream; Figure 1).

The relationship between hyporheic and overlying stream temperature may also vary seasonally. At site 1302, hyporheic and surface stream temperatures converged towards the end of the season (Figure 1), when discharge was at its lowest. This is likely due to the fact that, as the summer progresses and the water level decreases, hyporheic upwellings account for a larger proportion of total streamflow. As a result, the hyporheic temperature regime controls the surface temperature regime to a greater extent. This pattern may vary from year to year. The data we present here represent a single year (2022). In years with lower streamflow discharges, or when the low-flow season is more prolonged, the influence of hyporheic flows on stream temperatures may be correspondingly greater.

Based on the patterns we observed, we grouped the six study sites into three hyporheic temperature categories: cold, cool, and ambient. The cold category is represented by the one site where hyporheic temperatures were consistently colder than the overlying surface stream temperature during the low-flow season (1316). At site 1316, hyporheic temperatures averaged 11.7 °C and never exceeded 13.0 °C, while surface stream temperatures averaged 18 °C (Figure 1). The cool category denotes sites where hyporheic temperatures were variable but more moderate than overlying surface stream temperatures (1302 and 1306), and the ambient category denotes sites where hyporheic temperatures were not cooler or more stable than overlying surface stream temperatures (1312, 1313, and 2124).

The cold, cool, and ambient categories also serve to characterize hyporheic temperature in terms of daily maxima (Figure 2). Results from pairwise t-tests indicate that daily maximum temperatures were significantly cooler in the hyporheic zone, relative to the overlying surface stream, at each of the cold- and cool-classified sites. During the summer low-flow period, when surface stream temperatures warmed to approximately 20 °C on average, the maximum hyporheic temperature was approximately 18 °C at site 1302 (mean difference = -2.00 °C, $t_{32(1)} = -8.8$, $p < 0.001$), 18 °C at site 1306 (mean difference = -1.64 °C, $t_{20(1)} = -7.7$, $p < 0.001$), and 11.8 °C at site 1316 (mean difference = -8.34 °C, $t_{34(1)} = -23.5$, $p < 0.001$). In contrast, there were no significant differences between hyporheic and surface maxima at any of the ambient-classified sites (site 1312: mean difference = 0.14 °C, $t_{34(1)} = 2.9$, $p = 0.997$; site 1313: mean difference = 0.01 °C, $t_{34(1)} = 2.2$, $p = 0.982$; site 2124: mean difference = 0.01 °C, $t_{36(1)} = 1.6$, $p = 0.945$). Results for 7DADM were almost identical (see Supplementary Materials, Table S1), which suggests that the observed patterns were likely driven by season-long conditions rather than a few extreme temperature days.

These differences have potentially important implications for the provision of cool-water refuge for salmon. In Pacific Northwest rivers, a cool-water refuge is generally defined as a local-scale area or patch ≥ 2 °C cooler than the surrounding water (Torgersen et al. 2012). This distinction might not be meaningful in cases where the surrounding water temperature is > 2 °C above the threshold for adverse effects to salmon. Still, the patterns observed in this study suggest that the differences between hyporheic and surface temperatures may align with the difference between adverse and non-adverse conditions. For early Chinook Salmon, temperatures ≥ 19 °C can create thermal blockages, causing fish to cease upriver movement and seek shelter, which could disrupt coordinated arrival at spawning grounds or prevent spawning altogether (Richter and Kolmes 2005, McCullough et al. 2001). In the SF Nooksack, when daily maximum surface stream temperatures are above this threshold, hyporheic upwellings at cold- and cool-classified sites deliver water temperatures that may provide suitable refuge until seasonal cooling occurs and migration can resume.

As with daily maxima, diel variation in temperature was lower at cold- and cool-classified sites, but not at ambient-classified sites (Figure 3). Pairwise t-test results for the daily temperature range indicate that hyporheic ranges were significantly smaller at site 1302 (mean difference = -1.52 °C, $t_{32(1)} = -10.3$, $p < 0.001$), site 1306 (mean difference = -2.90 °C, $t_{20(1)} = -12.7$, $p < 0.001$), and site 1316 (mean difference = -3.69 °C, $t_{34(1)} = -20.9$, $p < 0.001$). In contrast, there were no significant differences between hyporheic and surface ranges at any of the ambient-classified sites (site 1312: mean difference = 0.12 °C, $t_{34(1)} = 2.6$, $p = 0.994$; site 1313: mean difference = -0.003 °C, $t_{34(1)} = -0.3$, $p = 0.381$; site 2124: mean difference = -0.012 °C, $t_{36(1)} = -1.5$, $p = 0.078$).

The patterns we observed were likely not confounded by variations in sampling depth or upwelling potential. Piezometer installation depths ranged from 30.5 to 37.5 cm among sites (Table 1), but regression analysis indicates no significant influence of installation depth on any response variable. Similarly, although the magnitude of upwelling potential (VHG) ranged from 0.25 to 2.5 (Table 1), VHG had no significant influence on any response variable (see Supplementary Materials, Table S2).

The differences in the hyporheic-surface stream temperature relationship observed among our study sites are likely driven by differences in the characteristics of the hyporheic flow paths that feed the upwellings. Hyporheic temperatures are largely governed by surface stream and groundwater temperatures, and by the degree of mixing between surface water and groundwater. This mixing is controlled by the interplay of channel morphology, gradient, sediment texture and hydraulic conductivity, as well as large-scale variations in topography, soil characteristics, and geology (Harvey and Bencala 1993, Olson 1995, Valett et al. 1996, Edwards 1998, Hester et al. 2017). Hyporheic temperatures may also be influenced by conductive heat exchange, which is controlled by sediment texture, thermal conductivity, and streambed heat capacity, as well as the depth, length, and residence time of the hyporheic flowpath (Beach and Peterson 2013, Bastola and Peterson 2016). The influence of surface water is generally attenuated with increasing depth and distance from downwelling locations. As a result, deeper and longer flow paths tend to be more thermally stable, remaining cooler during the summer low-flow season, when river temperatures tend to be at their warmest (Edwards 1998, Dogwiler and Wicks 2006, Fernald et al. 2006).

Hyporheic flow rates may also play a role, as flow paths with greater discharges may be more likely to affect surface temperatures at upwelling sites (Fernald et al. 2006, Arrigoni et al. 2008). Our study sites are all on the same aquifer (Gendaszek 2014) and experience similar surface temperatures (Figure 1), but different sites feature different hyporheic flowpaths that originate at different downwelling locations and vary from one another in terms of length, depth and flow rate. The upwellings observed at cool-classified sites (1302 and 1306) likely arise from flow paths that are longer or deeper or carry greater discharge, in comparison with the flow paths affecting the ambient-classified sites (1312, 1313, and 2124). The cold-classified site (1316) appears to be most strongly influenced by groundwater. This may be due to greater thermal conduction between hyporheic flows and adjacent groundwater (Menichino and Hester 2014) or greater flux of groundwater upwelling (Conant 2004, Schmidt et al. 2006), both of which may vary as a function of reach-scale heterogeneities in hydraulic head and hydraulic conductivity. The fine spatial scales at which we observed these heterogeneities (< 0.5 km between sites) are consistent with what has been reported elsewhere (e.g., Ebersole et al. 2003, Conant 2004).

Reach-scale variations in channel geomorphology may predict variations in hyporheic flow paths among study sites. Channel geomorphology impacts water depth and velocity and may exert a significant impact on the location and magnitude of hyporheic exchange, as well as the depths and flow rates of hyporheic flow paths. As illustrated in Figure 4, the cold and cool hyporheic sites at Nesset's Reach all occur where the riffle at the head of the log jam-formed pool is immediately below another pool, whereas the ambient sites all occur where the riffle is immediately below a run (i.e., an intermediate channel feature that is deeper and slower than a riffle but shallower and swifter than a pool; Fitzpatrick et al. 1998). This pattern aligns with the findings of previous studies (Fernald et al. 2006, Gariglio et al. 2013): When a pool transitions to a riffle, the spatial gradient in depth and velocity is steep, which forces more water down into the hyporheic zone, resulting in greater hyporheic flow and deeper flow paths downstream. In contrast, when a run transitions into a riffle, the spatial gradient in depth and velocity is less steep, resulting in diminished and shallower hyporheic flows. Consequently, the temperature of hyporheic upwellings may be determined in large part by specific combinations of channel geomorphic units upstream. Spatial configurations of channel geomorphic units may vary from year to year. In alluvial rivers, winter high flows can re-arrange streambed materials and re-shape channel morphology (Bierman and Montgomery 2014). As a result, the locations of cool flow paths may change from year to year within a reach, although the installation of engineered log jams can help stabilize pool locations to some extent.

The hyporheic temperatures presented here were measured in a single piezometer per site. Hyporheic flows can be complex, with flow paths of varying length, depth and point of origin occurring within close proximity to one another (Edwards 1998). At each of our sites, we installed the piezometer to capture hyporheic flows upwelling into the pool, but we have not captured the full range of flow paths that may be influencing each site. Nonetheless, our findings conservatively demonstrate the heterogeneity in hyporheic temperature regimes that may exist within a reach.

Conclusions and Recommendations

The findings of this research demonstrate that summertime hyporheic temperatures are not uniformly cooler or more stable than those of the overlying surface stream, and that hyporheic temperature regimes can vary significantly over relatively fine spatial scales beneath a reach of stream (i.e., within 0.5 km). Our findings also suggest that this variability may be largely driven by patterns of channel geomorphology.

These findings have potentially important implications for salmon habitat restoration strategies in thermally-impaired rivers. For projects that seek to promote cool-water refuge by preserving or enhancing hyporheic upwellings, or by locating holding water in areas that receive cool water from hyporheic upwellings, success may depend on locating cool, thermally stable flow paths. Mapping subsurface temperatures can be time- and labor-intensive, but our research suggests that potentially advantageous sites may be identified using more easily obtained habitat mapping data. Habitat managers can identify pool-riffle sequences where spatial gradients in depth and velocity are steep and then undertake targeted investigations of hyporheic and groundwater temperatures beneath those sequences. In cases where engineered log jams are used to create scour pools and promote hyporheic upwellings, cooler upwellings might be promoted by closer spacing between log jams. The design and configuration of the log jams may also play a role. In particular, the extent to which the structure spans the channel and the proportion of flow depth that is blocked may interact with channel conditions (e.g., gradient, substrate texture, ambient groundwater discharge) to influence the lengths and depths of hyporheic flow paths and rates of upwelling (Hester and Doyle 2008, Sawyer and Cardenas 2012, Sawyer et al. 2012).

It is important to recognize that hyporheic temperatures are not the only factor to consider with regard to the use of upwellings for providing cool-water refuge in thermally-impaired streams. Among other water quality parameters, dissolved oxygen concentrations may influence habitat quality. Since longer flow paths generally feature lower concentrations of dissolved oxygen as well as more stable temperatures (Edwards 1998, Fernald et al. 2006), each flow path likely has an optimal length whereby downstream upwellings are maximally cool and stable but retain adequate dissolved oxygen to support the metabolic requirements of target species. Moreover, where pools receive optimal hyporheic upwellings, mixing lengths may influence the quality of the resulting cool-water refuge habitat. Temperatures are likely to remain cooler at the bottoms of pools in areas where mixing is inhibited by structural features such as logs or gravel accumulations that deflect the main flow away from the pool (Keller and Hofstra 1983), or where pools stratify vertically (Tate et al. 2007). Site-specific investigations will be necessary to identify optimal flow path lengths and guide the location and design of engineered log jams.

Habitat restoration through engineered log jam construction can be a valuable tool for helping salmon and other thermally-sensitive fishes persist in thermally-impaired streams. Deep pools such as those created or enhanced by engineered log jams can provide refuge in various ways. Deep pools are more likely to stay cool in summer due to their relatively high thermal inertia and shading by LWD accumulations. Pools also provide energetically-favorable holding water that allows salmon to offset the energetic costs of elevated water temperatures. These benefits may be compounded where pools receive cool-water inputs from hyporheic upwellings. With thoughtful design and site selection guided by targeted, site-specific baseline data, such upwellings can be exploited to create effective refuge habitat and promote climate adaptation in salmon populations and the communities that depend on them.

Acknowledgements

This research was conducted within the ancestral homelands of the Coast Salish Peoples, who have lived in the Salish Sea basin since time immemorial. We express our deepest respect and gratitude to our Indigenous neighbors, the Lummi Nation and Nooksack Tribe, for their enduring care and protection of our shared lands and waterways. We feel honored to share this land and help support the recovery of Chinook Salmon. We also thank Mike Maudlin, Treva Coe, Kelley

Turner, Nathan Rice, and Alex Levell for their valuable contributions to the development of this project; Valerie Lloyd and Lawson Curtis for logistical support; Samantha Lopez for field assistance; Audrey Salerno for help with data analysis; and the associate editor and three anonymous reviewers for constructive suggestions that improved the manuscript. This research was funded by a Washington Sea Grant award (R/HCE-17) to James Helfield and a U.S. Geological Survey Northwest Climate Adaptation Science Center award (G17AC00218) to Sydney Jantsch.

Conflict of Interest

The authors declare that the research was conducted in the absence of any commercial or financial relationships that could be construed as a potential conflict of interest.

Data Availability Statement

The datasets used in this study can be found in repository in the Department of Environmental Sciences at Western Washington University.

Author Contributions

SJ: conceptualization, methodology, fieldwork, data analysis, visualization, writing—first draft, project administration, funding acquisition; JMH: conceptualization, methodology, fieldwork, writing—review and editing, supervision, funding acquisition; LB: methodology, supervision, writing—review and editing; KLS: methodology, supervision, writing—review and editing; AGB: methodology, data analysis, visualization, supervision.

References Cited

Arrigoni AS, Poole GC, Mertes LAK, O'Daniel SJ, Woessner WW, Thomas SA. 2008. Buffered, lagged or cooled? Disentangling hyporheic influences on temperature cycles in stream channels. Water Resources Research 44:W09418.

Bastola H, Peterson EW. 2016. Heat tracing to examine seasonal groundwater flow beneath a low-gradient stream in rural central Illinois, USA. Hydrogeology 24:181–194.

Baxter CV, Hauer FR, Woessner WW. 2003. Measuring groundwater–stream water exchange: new techniques for installing minipiezometers and estimating hydraulic conductivity. Transactions of the American Fisheries Society 132:493–502.

Beach V, Peterson EW. 2013. Variation of hyporheic temperature profiles in a low gradient third-order agricultural stream — a statistical approach. Open Journal of Modern Hydrology 3:55–66.

Beechie TJ, Sibley TH. 1997. Relationships between channel characteristics, woody debris, and fish habitat in northwestern Washington streams. Transactions of the American Fisheries Society 126:217–229.

Benda SE, Naughton GP, Caudill CC, Kent ML, Schreck CB. 2015. Cool, pathogen-free refuge lowers pathogen-associated prespawn mortality of Willamette River Chinook Salmon. Transactions of the American Fisheries Society 144:1159–1172.

Bierman PR, Montgomery DR. 2014. Key Concepts in Geomorphology. W.H. Freeman and Company Publishers, New York.

Bilski RL, Wheaton JM, Merz JE. 2022. Effects of in-channel structure on Chinook Salmon spawning habitat and embryo production. Water 14:83. DOI:10.3390/w14010083

Bjornn TC, Reiser DW. 1991. Habitat requirements of salmonids in streams. American Fisheries Society Special Publication 19:83–138.

Booker DJ, Whitehead AL. 2022. River water temperatures are higher during lower flows after accounting for meteorological variability. River Research and Applications 38:3–22.

Bowen L, von Biela VR, McCormick SD, Regish AM, Waters SC, Durbin-Johnson B, Britton M, Settles ML, Donnelly DS, Laske SM, Carey MP, Brown RJ, Zimmerman, CE. 2020. Transcriptomic response to elevated water temperatures in adult migrating Yukon River Chinook Salmon (*Oncorhynchus tshawytscha*). Conservation Physiology 8(1): coaa084.

Burkholder BK, Grant GE, Haggerty R, Khangaonkar T, Wampler PJ. 2008. Influence of hyporheic flow and geomorphology on temperature of a large, gravel-bed river, Clackamas River, Oregon, USA. Hydrological Processes 22:941–953.

Butcher JB, Faizullabhoy M, Nicholas H, Cada P, Kennedy JT. 2016. Quantitative assessment of temperature sensitivity of the South Fork Nooksack River under future climates using QUAL2Kw. U.S. Environmental Protection Agency, EPA/600/R-14/233, Washington, DC.

Carothers C, Black J, Langdon SJ, Donkersloot R, Ringer D, Coleman J, Gavenus ER, Justin W, Williams M, Christiansen F, Samuelson J, Stevens C, Woods B, Clark SJ, Clay PM, Mack L, Raymond-Yakoubian J, Sanders AA, Stevens BL, Whiting A. 2021. Indigenous peoples and salmon stewardship: a critical relationship. Ecology and Society 26:16.

Cederholm CJ, Houston DB, Cole DL, Scarlett WJ. 1989. Fate of Coho Salmon (*Oncorhynchus kisutch*) carcasses in spawning streams. Canadian Journal of Fisheries and Aquatic Sciences 46:1347–1355.

Coe T. 2019. Quality assurance project plan for implementation and effectiveness monitoring of Nooksack River Watershed habitat restoration projects. Revision 1: June 30, 2019. Nooksack Indian Tribe Natural Resources Department, Deming, WA.

Conant B, Jr. 2004. Delineating and quantifying ground water discharge zones using streambed temperatures. Ground Water 42:243–257.

Connor WP, Tiffan KF, Chandler JA, Rondorf DW, Arnsberg BD, Anderson KC. 2019. Upstream migration and spawning success of Chinook Salmon in a highly developed, seasonally warm river system. Reviews in Fisheries Science & Aquaculture 27:1–50.

Cramer ML (editor). 2012. Stream habitat restoration guidelines. Washington Departments of Fish and Wildlife, Natural Resources, Transportation and Ecology, Washington State Recreation and Conservation Office, Puget Sound Partnership, and U.S. Fish and Wildlife Service, Olympia, WA.

Dahm CN, Valett HM. 1996. Hyporheic Zones. *In* FR Hauer and GA Lamberti (editors), Methods in Stream Ecology. Academic Press, San Diego, CA. Pp. 107–119.

[DFO] Fisheries and Oceans Canada. 2018. Wild salmon policy 2018-2022 implementation plan. Fisheries and Oceans Canada, Pacific Region, Victoria, BC.

Dogwiler TJ, Wicks CM. 2006. Thermal variations in the hyporheic zone of a karst stream. International Journal of Speleology 35:59–66.

Ebersole JL, Liss WJ, Frissell CA. 2001. Relationship between stream temperature, thermal refugia and Rainbow Trout *Oncorhynchus mykiss* abundance in arid-land streams in the northwestern United States. Ecology of Freshwater Fish 10:1–10.

Ebersole JL, Liss WJ, Frissell CA. 2003. Thermal heterogeneity, stream channel morphology, and salmonid abundance in northeastern Oregon streams. Canadian Journal of Fisheries and Aquatic Sciences 60:1266–1280.

Edwards RT. 1998. The Hyporheic Zone. *In* RJ Naiman and RE Bilby (editors), River Ecology and Management: Lessons from the Pacific Coastal Ecoregion. Springer-Verlag, New York. Pp. 399–429.

Elliott JM. 2000. Pools as refugia for Brown Trout during two summer droughts: trout responses to thermal and oxygen stress. Journal of Fish Biology 56:938–948.

Fernald AG, Landers DH, Wigington PJ, Jr. 2006. Water quality changes in hyporheic flow paths between a large gravel bed river and off-channel alcoves in Oregon, USA. River Research and Applications 22:1111–1124.

Fitzpatrick FA, Waite IR, D'Arconte PJ, Meader MR, Maupin MA, Gurtz ME. 1998. Revised methods for characterizing stream habitat in the national water-quality assessment program. U.S. Geological Survey Water-Resources Investigations Report 98-4052, Raleigh, NC.

Ford JK, Ellis GM, Olesiuk PF, Balcomb KC. 2010. Linking killer whale survival and prey abundance: food limitation in the oceans' apex predator? Biology Letters 6:139–142.

Gariglio FP, Tonina D, Luce CH. 2013. Spatiotemporal variability of hyporheic exchange through a pool-riffle-pool sequence. Water Resources Research 49:7185–7204.

Gendaszek A, 2014. Hydrogeologic framework and groundwater/surface-water interactions of the South Fork Nooksack River basin, northwestern Washington. U.S. Geological Survey Scientific Investigations Report 2014–5221, Reston, VA.

Grah O, O'Neil H, Coe T. 2017. South Fork Nooksack River watershed conservation plan. Nooksack Indian Tribe Natural Resources Department, South Fork Nooksack Watershed Conservation Plan, Deming, WA.

Gregory SV, Boyer KL, Gurnell AM (editors). 2003. The Ecology and Management of Wood in World Rivers. American Fisheries Society Symposium 37, Bethesda, MD.

Gustafson RG, Waples RS, Myers JM, Weitkamp LA, Bryant GJ, Johnson OW, Hard JJ. 2007. Pacific salmon extinctions: quantifying lost and remaining diversity. Conservation Biology 21:1009–1020.

Harvey JW, Bencala KE. 1993. The effect of streambed topography on surface-subsurface water exchange in mountain catchments. Water Resources Research 29:89–98.

Hashim WA, Bresler H. 2005. Washington's water quality management plan to control nonpoint source pollution. Washington Department of Ecology Publication No. 05-10-027, Olympia, WA.

Helfield JM, Naiman RJ. 2006. Keystone interactions: salmon and bear in riparian forests of Alaska. Ecosystems 9:167–180.

Hester ET, Doyle MW. 2008. In-stream geomorphic structures as drivers of hyporheic exchange. Water Resources Research 44:W03417. DOI:10.1029/2006WR005810

Hester ET, Doyle MW, Poole GC. 2009. The influence of in-stream structures on summer water temperatures via induced hyporheic exchange. Limnology and Oceanography 54:355–367.

Hester ET, Cardenas MB, Haggerty R, Apte SV. 2017. The importance and challenge of hyporheic mixing. Water Resources Research 53:3565–3575.

Hilderbrand GV, Schwartz CC, Robbins CT, Jacoby ME, Hanley TA, Arthur SM, Servheen C. 1999. The importance of meat, particularly salmon, to body size, population productivity, and conservation of North American brown bears. Canadian Journal of Zoology 77:132–138.

Hinch SG, Martins EG. 2011. A review of potential climate change effects on survival of Fraser River Sockeye Salmon and an analysis of interannual trends in en route loss and pre-spawn mortality. Cohen Commission Technical Report 9, Vancouver, B.C.

Kasahara T, Wondzell SM. 2003. Geomorphic controls on hyporheic exchange flow in mountain streams. Water Resources Research 39:1005. DOI:10.1029/2002WR001386

Keller EA, Hofstra TD. 1983. Summer cold pools in Redwood Creek near Orick, California, and their importance as habitat for anadromous salmonids. *In* Proceedings of First Biennial Conference of Research in California National Parks. U.S. National Park Service, Cooperative Park Studies Unit, Davis, CA. Pp. 221–224.

Lackey RT. 2022. The great Pacific Northwest salmon conundrum. Water Resources IMPACT. 24:5–8.

Lundberg J, Moberg F. 2003. Mobile link organisms and ecosystem functioning: implications for ecosystem resilience and management. Ecosystems 6:87–98.

Manly BFJ. 2007. Randomization, Bootstrap and Monte Carlo Methods in Biology (3rd ed.). Chapman & Hall/CRC Press, Boca Raton, FL.

Maudlin M, Coe T, Currence N, Hansen J. 2002. South Fork Nooksack River Acme-Saxon Reach restoration planning: analysis of existing information and preliminary recommendations. Lummi Nation Natural Resources Department, Bellingham, WA.

McCullough D, Spalding S, Sturdevant D, Hicks M. 2001. Issue paper 5: summary of technical literature examining the physiological effects of temperature on salmonids. U.S. Environmental Protection Agency Report EPA-910-D-01-005, Region 10, Seattle, WA.

Menichino GT, Hester ET. 2014. Hydraulic and thermal effects of in-stream structure-induced hyporheic exchange across a range of hydraulic conductivities. Water Resources Research 50:4643–4661.

Mote PW, Parson EA, Hamlet AF, Keeton WS, Lettenmaier D, Mantua N, Miles EL, Peterson DW, Peterson DL, Slaughter R, Snover AK. 2003. Preparing for climate change: the water, salmon, and forests of the Pacific Northwest. Climate Change 61:45–88.

Mutz M, Kalbus E, Meinecke S. 2007. Effect of instream wood on vertical water flux in low-energy sand bed flume experiments. Water Resources Research 43:W10424. DOI: 10.1029/2006WR005676

Newell D. 1994. Tangled Webs of History: Indians and the Law in Canada’s Pacific Coast Fisheries. University of Toronto Press, Toronto, Ont.

[NOAA] National Oceanic and Atmospheric Administration. 2015. Status review update for Pacific salmon and Steelhead listed under the Endangered Species Act: Pacific Northwest. NOAA Technical Memorandum NMFS-NWFSC-113. Northwest Fisheries Science Center, Seattle, WA.

[NNR] Nooksack Indian Tribe Natural Resources Department. 2012. South Fork Nooksack (Nuxw7íyem) Nesset Reach design. Salmon Recovery Funding Board Project #12-1511, Washington State Recreation and Conservation Office, Olympia, WA. https://srp.rco.wa.gov/project/360/17944 (accessed 22 June 2023).

[NNR] Nooksack Indian Tribe Natural Resources Department. 2015. South Fork Nooksack (Nuxw7íyem) Nesset phase 1 restoration. Salmon Recovery Funding Board Project #15-1283. Washington State Recreation and Conservation Office, Olympia, WA. https://srp.rco.wa.gov/project/360/29581 (accessed 18 November 2022).

[NNR] Nooksack Indian Tribe Natural Resources Department. 2016. South Fork Nooksack (Nuxw7íyem) Nesset phase 2 restoration. Salmon Recovery Funding Board Project #16-2049. Washington State Recreation and Conservation Office, Olympia, WA. https://srp.rco.wa.gov/project/360/80475 (accessed 18 November 2022).

Olson PL. 1995. Shallow subsurface flow systems in a montane terrace-floodplain landscape: Sauk River, North Cascades, Washington. Ph.D. Dissertation, University of Washington, Seattle, WA.

Pelto MS, Dryak M, Pelto J, Matthews T, Perry LB. 2022. Contribution of glacier runoff during heat waves in the Nooksack River basin USA. Water 14:1145.

Poole, GC, Berman CH. 2001. An ecological perspective on in-stream temperature: natural heat dynamics and mechanisms of human-caused thermal degradation. Environmental Management 27:787–802.

R Core Team. 2023. R: A language and environment for statistical computing. R Foundation for Statistical Computing, Vienna, Austria. https://www.R-project.org/ (accessed 20 June 2024).

Richter A, Kolmes SA. 2005. Maximum temperature limits for Chinook, Coho, and Chum Salmon, and Steelhead Trout in the Pacific Northwest. Reviews in Fisheries Science 13:23–49.

Roni P, Hanson K, Beechie T. 2008. Global review of the physical and biological effectiveness of stream habitat rehabilitation techniques. North American Journal of Fisheries Management 28:856–890.

Sawyer AH, Cardenas MB. 2012. Effect of experimental wood addition on hyporheic exchange and thermal dynamics in a losing meadow stream. Water Resources Research 48:W10537. DOI:10.1029/2011WR011776

Sawyer AH, Cardenas MB, Buttles J. 2012. Hyporheic temperature dynamics and heat exchange near channel-spanning logs. Water Resources Research 48:W01529. DOI:10.1029/2011WR011200

Schmidt C, Bayer-Raich M, Schirmer M. 2006. Characterization of spatial heterogeneity of groundwater-stream water interactions using multiple depth streambed temperature measurements at the reach scale. Hydrology and Earth System Sciences Discussions 3:1419–1446.

Schoonmaker PK, Gresh T, Lichatowich J, Radtke HD. 2003. Past and Present Pacific salmon Abundance: Bioregional Estimates for Key Life History Stages. *In* JG Stockner (editor), Nutrients in Salmonid Ecosystems: Sustaining Production and Biodiversity. American Fisheries Society, Bethesda, MD. Pp. 33–40.

Soicher A, Coe T, Currence N. 2006. South Fork Nooksack River Acme-Confluence Reach restoration planning: analysis of existing information and preliminary restoration strategies. IAC #02-1500N Final Report. Nooksack Tribe Natural Resources Department, Deming, WA.

Tate KW, Lancaster DL, Lile DF. 2007. Assessment of thermal stratification within stream pools as a mechanism to provide refugia for native trout in hot, arid rangelands. Environmental Monitoring and Assessment 124:289–300.

Tonina D, Buffington JM. 2007. Hyporheic exchange in gravel bed rivers with pool-riffle morphology: laboratory experiments and three-dimensional modeling. Water Resources Research 43:W01421. DOI: 10.1029/2005WR004328

Torgersen CE, Ebersole JE, Keenan DM. 2012. Primer for identifying cold-water refuges to protect and restore thermal diversity in riverine landscapes. U.S. Environmental Protection Agency Report EPA 910-C-12-001, Region 10, Seattle, WA.

[USEPA] U.S. Environmental Protection Agency. 2016a. Final project report: EPA Region 10 climate change and TMDL pilot—South Fork Nooksack River, Washington. EPA/600/R-17/281. National Health and Environmental Effects Research Laboratory, Western Ecology Division, Corvallis, OR.

[USEPA] U.S. Environmental Protection Agency. 2016b. Qualitative assessment: evaluating the impacts of climate change on Endangered Species Act recovery actions for the South Fork Nooksack River, Washington. EPA/600/R-16/153. National Health and Environmental Effects Research Laboratory, Western Ecology Division, Corvallis, OR.

[USEPA] U.S. Environmental Protection Agency. 2021. Impaired waters and TMDLs in Region 10. https://www.epa.gov/tmdl/impaired-waters-and-tmdls-region-10 (accessed 11 March 2021).

[USGS] U.S. Geological Survey. 2024. SF Nooksack River at Saxon Bridge, WA – 12210000, October 1, 2021 – September 30, 2022. https://waterdata.usgs.gov/monitoring-location/12210000/#parameterCode=00060&startDT=2021-10-01&endDT=2022-09-30&showMedian=true (accessed 10 July 2024).

Valett HM, Morrice JA, Dahm CN, Campana ME. 1996. Parent lithology, surface-groundwater exchange, and nitrate retention in head water streams. Limnology and Oceanography 41:333–345.

van Vliet MTH, Ludwig F, Zwolsman JJG, Weedon GP, Kabat P. 2011. Global river temperatures and sensitivity to atmospheric warming and changes in river flow. Water Resources Research 47:W02544. DOI:10.1029/2010WR009198

von Biela VR, Bowen L, McCormick SD, Carey MP, Donnelly DS, Waters S, Regish AM, Laske SM, Brown RJ, Larson S, Zuray S, Zimmerman CE. 2020. Evidence of prevalent heat stress in Yukon River Chinook Salmon. Canadian Journal of Fisheries and Aquatic Sciences 77:1878–1892.

Willson MF, Gende SM, Marston BH. 1998. Fishes and the forest: expanding perspectives on fish-wildlife interactions. BioScience 48:455–462.

Wondzell SM, LaNier J, Haggerty R, Woodsmith RD, Edwards RT. 2009. Changes in hyporheic exchange flow following experimental wood removal in a small, low-gradient stream. Water Resources Research 45:W05406. DOI: 10.1029/2008WR007214

[WRIA 1 SRB] Water Resources Inventory Area 1 Salmon Recovery Board. 2005. Salmonid recovery plan, October 11, 2005, Bellingham, WA.

Yoder J, Raymond C. 2022. Climate change and stream flow: barriers and opportunities. Washington State Department of Ecology Water Resources Program Publication 22-11-029, Olympia, WA.

Submitted 30 July 2024

Accepted 14 April 2025

Figures

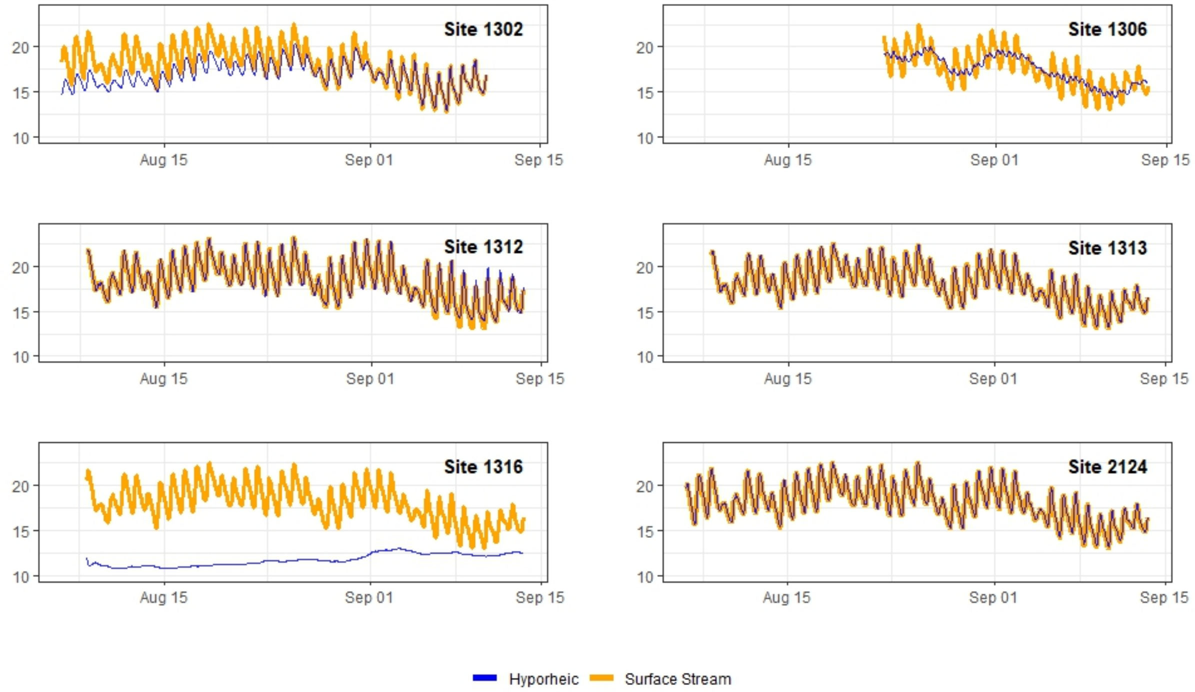

Figure 1. Hyporheic and surface stream temperatures at study sites in Nesset's Reach, South Fork Nooksack River, from August 6 to September 13, 2022.

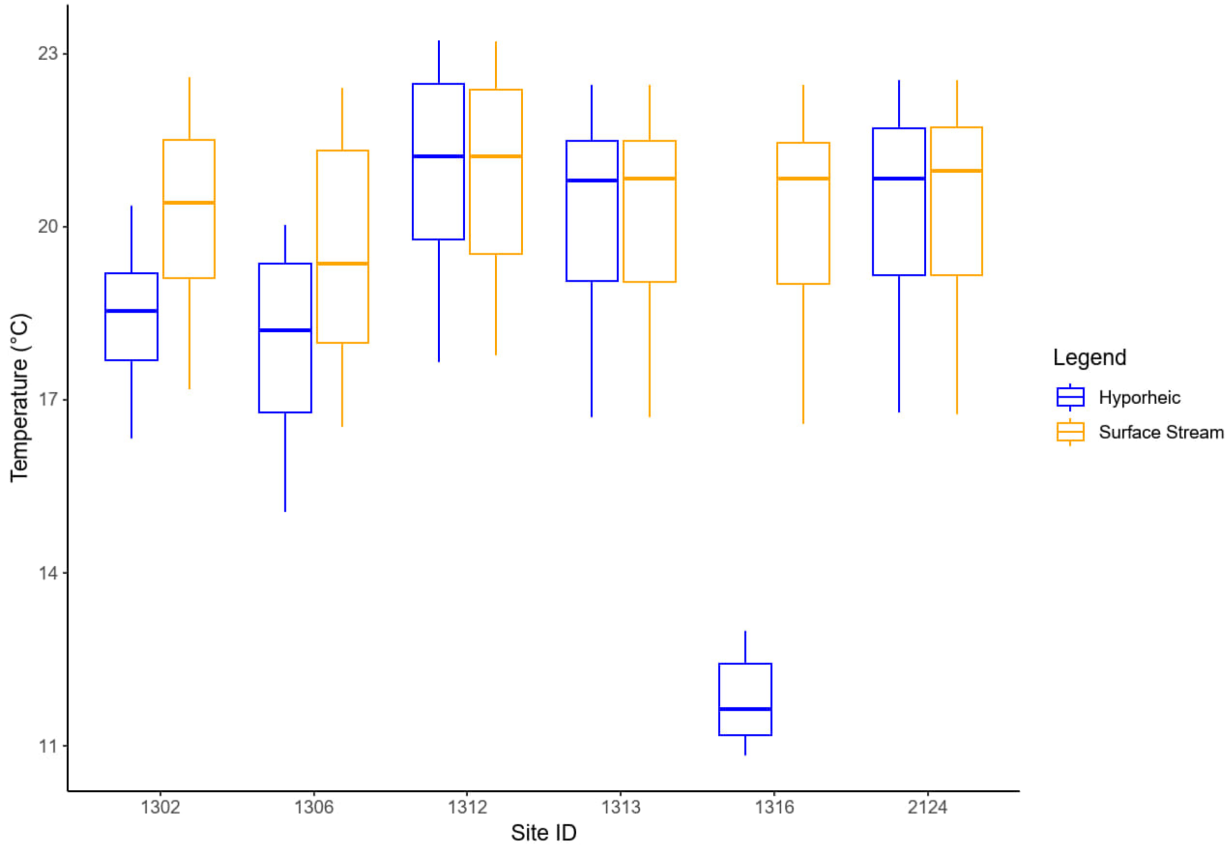

Figure 2. Boxplots of daily maximum hyporheic and surface stream temperatures at study sites in Nesset's Reach, South Fork Nooksack River, during the 2022 summer low-flow season (August 6 to September 13). The midline represents the median value, the box represents the interquartile range, and the whiskers represent 1.5 times the interquartile range.

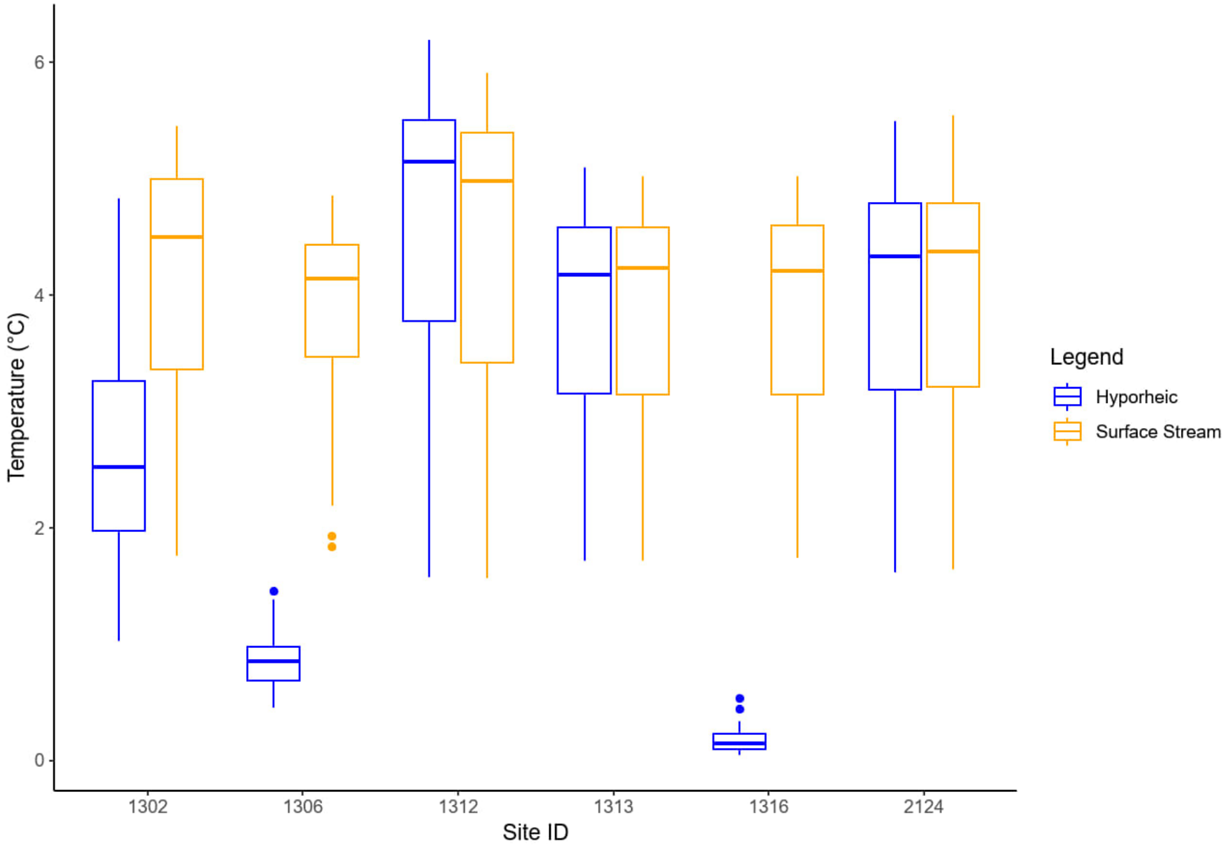

Figure 3. Boxplots of the daily range of hyporheic and surface stream temperatures at study sites in Nesset's Reach, South Fork Nooksack River, during the 2022 summer low-flow season (August 6 to September 13). The midline represents the median value, the box represents the interquartile range, the whiskers represent 1.5 times the interquartile range, and the dots represent outliers.

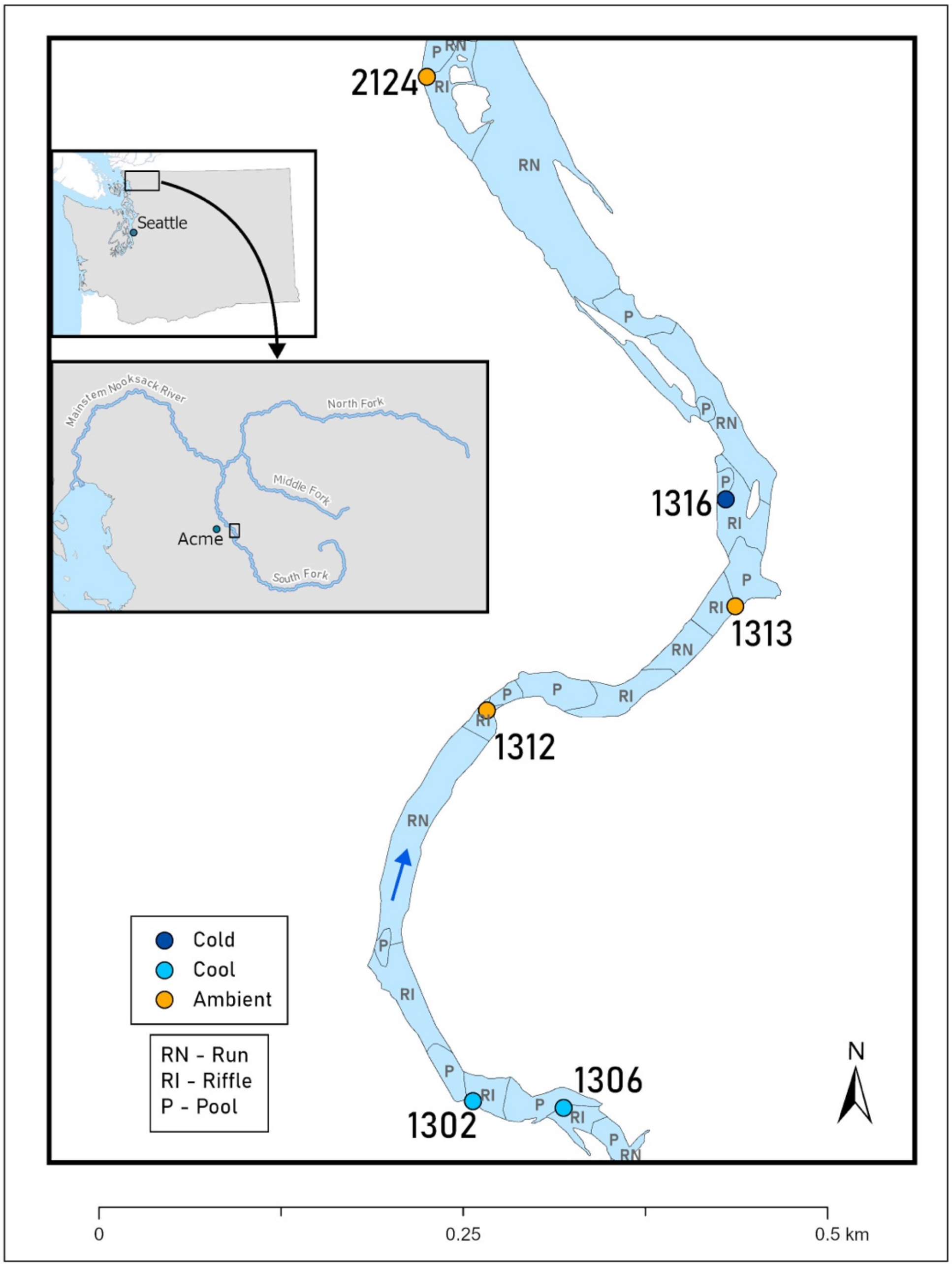

Figure 4. Study sites in Nesset's Reach, South Fork Nooksack River, identified by hyporheic temperature categories with surrounding channel geomorphic units. The blue arrow indicates the direction of river flow. The top inset map depicts the location of the Nooksack River in Washington State. The lower inset map shows the full extent of the Nooksack River, with Nesset's Reach highlighted.

Tables

Table 1. Locations and descriptions of study sites in Nesset's Reach, South Fork Nooksack River. Each site consists of a single engineered log jam and its associated wood-formed pool, with a riffle immediately upstream. Piezometers and temperature loggers were installed at the riffle tail/pool head. Residual pool depth was calculated as the difference between the maximum water depth within the pool and the water depth at the pool tailout. Upwelling potential was assessed in terms of vertical hydraulic gradient (VHG), a unitless measure of the pressure differential between the hyporheic zone at the piezometer location and the overlying surface stream.

Site ID	Location (latitude, longitude)	Year of log jam construction	Residual pool depth (m)	Piezometer installation depth (cm below streambed)	VHG
1302	(48.689145 °N, -122.165981 °W)	2016	1.34	37.5	+1.0
1306	(48.689115 °N, -122.165132 °W)	2016	1.89	30.5	+1.0
1312	(48.691559 °N, -122.165912 °W)	2016	0.76	36.75	+2.5
1313	(48.692227 °N, -122.163613 °W)	2016	>3.17	33.75	+1.5
1316	(48.692887 °N, -122.163720 °W)	2016	0.91	33	+1.0
2124	(48.695461 °N, -122.166573 °W)	2018	0.88	32.75	+0.25

Table 2. Results of permutation tests comparing surface stream temperatures and underlying hyporheic temperatures at each hour of the day at each study site. Data presented are the mean surface – hyporheic difference in temperature ($T_{diff.}$), where each temperature measurement represents the mean temperature in °C for that hour, averaged over all days in the sample period. Significant differences ($p < 0.05$) are highlighted and marked with asterisks.

	Site 1302		Site 1306		Site 1312		Site 1313		Site 1316		Site 2124	
Time	$T_{diff.}$	*p*	$T_{diff.}$	*p*	$T_{diff.}$	*p*	$T_{diff.}$	*p*	$T_{diff.}$	*p*	$T_{diff.}$	*p*
00:00	**.919**	**.019***	.226	.681	.143	.700	-.023	.942	**6.530**	**.001***	-.046	.903
01:00	**.814**	**.031***	-.124	.804	.144	.722	-.032	.927	**6.296**	**.001***	-.052	.883
02:00	.721	.075	-.448	.343	.127	.761	-.035	.928	**6.032**	**.001***	-.055	.875
03:00	.629	.090	-.730	.139	.109	.775	-.036	.917	**5.770**	**.001***	-.059	.863
04:00	.533	.165	-.980	.052	.085	.845	-.041	.923	**5.504**	**.001***	-.058	.879
05:00	.438	.265	**-1.193**	**.021***	.049	.908	-.048	.880	**5.235**	**.001***	-.061	.873
06:00	.348	.353	**-1.379**	**.011***	.012	.977	-.057	.877	**4.964**	**.001***	-.063	.855
07:00	.298	.406	**-1.542**	**.012***	-.018	.958	-.055	.880	**4.719**	**.001***	-.060	.882
08:00	.344	.286	**-1.632**	**.003***	-.034	.926	-.034	.938	**4.562**	**.001***	-.052	.886
09:00	.584	.069	**-1.553**	**.004***	-.039	.894	.017	.960	**4.595**	**.001***	-.006	.992
10:00	**.947**	**.001***	**-1.346**	**.012***	-.006	.983	.067	.843	**4.852**	**.001***	.033	.919
11:00	**1.423**	**.001***	-.918	.072	-.012	.962	.101	.765	**5.376**	**.001***	.082	.799
12:00	**1.947**	**.001***	-.367	.448	-.028	.920	.127	.712	**6.059**	**.001***	.105	.757
13:00	**2.360**	**.001***	.386	.449	-.002	.996	.145	.688	**6.807**	**.001***	.129	.703
14:00	**2.590**	**.001***	**1.198**	**.035***	-.034	.938	.131	.726	**7.557**	**.001***	.119	.711
15:00	**2.604**	**.001***	**1.678**	**.003***	-.089	.826	.071	.874	**8.001**	**.001***	.076	.846

16:00	**2.311**	**.001***	**1.948**	**.001***	-.246	.533	-.016	.975	**8.289**	**.001***	.007	.985
17:00	**1.977**	**.001***	**1.869**	**.003***	-.143	.725	-.064	.900	**8.212**	**.001***	-.050	.924
18:00	**1.614**	**.002***	**1.608**	**.006***	-.125	.757	-.104	.800	**7.920**	**.001***	-.085	.815
19:00	**1.310**	**.005***	**1.332**	**.018***	-.080	.850	-.097	.818	**7.509**	**.001***	-.109	.770
20:00	**1.170**	**.010***	**1.152**	**.042***	-.008	.986	-.052	.897	**7.208**	**.001***	-.092	.821
21:00	**1.069**	**.012***	.985	.068	.051	.924	-.038	.918	**6.973**	**.001***	-.065	.878
22:00	**.992**	**.010***	.761	.154	.112	.807	-.024	.959	**6.777**	**.001***	-.054	.896
23:00	**.928**	**.021***	.503	.329	.137	.776	-.020	.965	**6.578**	**.001***	-.049	.883

Jantsch S, Helfield JM, Bodensteiner L, Sobocinski KL, Bunn AG. 2025. A characterization of hyporheic temperatures with applications for salmon habitat restoration in a thermally impaired river. Northwest Science 98(2): *in press.*

Supplementary Materials

Table S1. Results of pairwise one-tailed t-tests comparing mean seven-day average of the daily maximum temperature (7DADM), averaged over all days in the sample period, between the hyporheic zone and overlying surface stream at study sites. Results presented include the test statistic (*t*), degrees of freedom (df), and p-value (*p*).

Site ID	Hyporheic temperature category	Sampling period	Mean hyporheic 7DADM (°C)	Mean surface stream 7DADM (°C)	Difference in means (°C)	*t*	df	*p*
1302	COOL	8/6/22 – 9/10/22	18.520	20.545	-2.02	-10.2	26	< 0.001
1306	COOL	8/22/22 – 9/13/22	18.089	19.698	-1.61	-22.5	14	< 0.001
1312	AMBIENT	8/8/22 – 9/13/22	21.315	21.223	0.09	3.4	28	0.999
1313	AMBIENT	8/8/22 – 9/13/22	20.475	20.461	0.013	3.4	28	0.999
1316	COLD	8/8/22 – 9/13/22	11.795	20.426	-8.63	-27.9	28	< 0.001
2124	AMBIENT	8/6/22 – 9/13/22	20.549	20.541	0.008	2.6	30	0.993

Table S2. Results of regression analyses assessing the effects of piezometer installation depth and vertical hydraulic gradient (VHG) on response variables. Response variables include the daily maximum temperature, the seven-day average of the daily maximum temperature (7DADM), and the daily temperature range. Results presented include the Adjusted R^2, F-statistic (*F*), degrees of freedom (df), and p-value (*p*).

	Installation depth				VHG			
Response variable	R^2	*F*	df	*p*	R^2	*F*	df	*p*
Daily maximum	-0.152	0.340	1,4	0.591	-0.150	0.348	1,4	0.587
7DADM	-0.152	0.341	1,4	0.590	-0.149	0.353	1,4	0.584
Daily range	0.062	1.329	1,4	0.313	-0.087	0.599	1,4	0.482